

EZH1 and EZH2 cogovern histone H3K27 trimethylation and are essential for hair follicle homeostasis and wound repair

Elena Ezhkova,^{1,3} Wen-Hui Lien,¹ Nicole Stokes,¹ H. Amalia Pasolli,¹ Jose M. Silva,² and Elaine Fuchs^{1,4}

¹Howard Hughes Medical Institute, Laboratory of Mammalian Cell Biology and Development, The Rockefeller University, New York, New York 10065, USA; ²Institute for Cancer Genetics, Irving Cancer Research Center, Columbia University Medical School, New York, New York 10032, USA

Polycomb protein group (PcG)-dependent trimethylation on H3K27 (H3K27me3) regulates identity of embryonic stem cells (ESCs). How H3K27me3 governs adult SCs and tissue development is unclear. Here, we conditionally target H3K27 methyltransferases *Ezh2* and *Ezh1* to address their roles in mouse skin homeostasis. Postnatal phenotypes appear only in doubly targeted skin, where H3K27me3 is abolished, revealing functional redundancy in EZH1/2 proteins. Surprisingly, while *Ezh1/2*-null hair follicles (HFs) arrest morphogenesis and degenerate due to defective proliferation and increased apoptosis, epidermis hyperproliferates and survives engraftment. mRNA microarray studies reveal that, despite these striking phenotypic differences, similar genes are up-regulated in HF and epidermal *Ezh1/2*-null progenitors. Featured prominently are (1) PcG-controlled nonskin lineage genes, whose expression is still significantly lower than in native tissues, and (2) the PcG-regulated *Ink4a/Inkb/Arf* locus. Interestingly, when EZH1/2 are absent, even though *Ink4a/Arf/Ink4b* genes are fully activated in HF cells, they are only partially so in epidermal progenitors. Importantly, transduction of *Ink4b/Ink4a/Arf* shRNAs restores proliferation/survival of *Ezh1/2*-null HF progenitors in vitro, pointing toward the relevance of this locus to the observed HF phenotypes. Our findings reveal new insights into Polycomb-dependent tissue control, and provide a new twist to how different progenitors within one tissue respond to loss of H3K27me3.

[Keywords: *Ezh1*; *Ezh2*; epigenetics; skin; stem cells]

Supplemental material is available for this article.

Received December 7, 2010; revised version accepted January 18, 2011.

Understanding how proliferation, apoptosis and differentiation are balanced in tissue development and homeostasis is important not only for uncovering key regulators that control tissue biology, but also for elucidating processes that, when altered, can lead to disease states such as cancer. Increasing evidence indicates that epigenetic chromatin modifications play critical roles in these processes. By changing chromatin structure, chromatin modifiers alter the accessibility of a gene to the transcriptional machinery and promote either its activation or its silencing.

Recent studies have revealed an important role for a chromatin regulator called the Polycomb group (PcG) complex in regulating normal tissue homeostasis and promoting cancer progression when awry (Sauvageau and

Sauvageau 2010). Polycomb proteins form chromatin remodeling complexes referred to as Polycomb-repressive complexes (PRCs) (Ringrose and Paro 2004). Comprised of EZH2, Eed, and Suz12, PRC2 is recruited to chromatin, where the catalytic component methyltransferase EZH2 catalyzes trimethylation on Lys 27 of histone H3 (H3K27me3) (Cao et al. 2002). This histone mark then provides a platform to recruit PRC1 (Cao et al. 2002; Min et al. 2003), which aids in Polycomb-mediated gene repression by mechanisms still unclear (Francis et al. 2004; Ringrose and Paro 2004; Sarma et al. 2008; Simon and Kingston 2009).

Genetic studies in *Drosophila* have long revealed an essential role for the PcG complex in repressing the Hox genes that pattern tissues in developing fly embryos (Lewis 1978; Simon and Kingston 2009). In vitro studies on cultured human embryonic stem cells (ESCs) have substantiated the evolutionary conservation of PcG proteins in repressing these key developmental genes, but in addition identify a much larger cohort of key differentiation genes as targets of this methylation mark (Boyer

³Present address: Department of Developmental and Regenerative Biology, Black Family Stem Cell Institute, Mount Sinai School of Medicine, 1428 Madison Ave., New York, NY 10029, USA.

⁴Corresponding author.

E-MAIL fuchslb@rockefeller.edu; FAX (212) 327-7954.

Article published online ahead of print. Article and publication date are online at <http://www.genesdev.org/cgi/doi/10.1101/gad.2019811>.

et al. 2006; Lee et al. 2006). Further chromatin analysis coupled with loss-of-function studies has led to a model whereby the mark might maintain the pluripotent state by repressing differentiation genes, but making the repressed state flexible by interacting with chromatin activators.

Most of what is known about the role of the PcG complex in mammalian tissues stems from ablation of *Bmi1*, encoding a component of the PRC1 complex. Mice lacking *Bmi1* succumb in early adult life due to defects in their hematopoietic and neuronal tissues. The loss seems to specifically affect the SCs, where compromise of self-renewal has been attributed to derepression of the *Ink4a/Arf* locus (Molofsky et al. 2003; Park et al. 2003). Interestingly, however, the loss of *Bmi1* does not affect the H3K27me3 histone mark (Cao et al. 2005), raising questions as to the extent to which PcG chromatin repression is crippled by this mutation, and whether the PRC1 complex may function in additional ways.

The role for the H3K27me3 mark in adult mammalian tissues has remained elusive, and has been only partially resolved by conditional targeting of *Ezh2*. Loss of EZH2 in a diverse array of tissues—including epidermis, pancreas, blood, and cerebral cortex—has yielded surprisingly mild phenotypes (Pereira et al. 2010; Su et al. 2003, 2005; Chen et al. 2009; Ezhkova et al. 2009). In the pancreas, loss of EZH2 results in mild diabetes, associated with an increase in p16^{INK4a} and p19^{Arf} (Chen et al. 2009). In the brain, loss of EZH2 shifted the balance of cortical progenitors from self-renewal to differentiation, similar to loss of *Bmi1* (Pereira et al. 2010). In embryonic skin, loss of EZH2 accelerated embryonic skin development by derepressing epidermal differentiation genes in the basal cell progenitors, without globally derepressing other differentiation pathways controlled by PcG (Ezhkova et al. 2009). Importantly, despite the apparent loss of H3K27me3 marks in embryonic basal cells, other skin epithelial cells appeared oblivious to EZH2 loss, displaying what appeared to be a full complement of H3K27me3 marks. Moreover, by birth, this histone mark reappeared in the basal cells. The incomplete loss of H3K27me3, coupled with the relatively mild defects in tissues lacking EZH2, raises the possibility of redundancy and precludes definitive statements about the role of this key epigenetic mark in tissue development and homeostasis.

Recent studies on cultured ESCs have shown that EZH1, a homolog of EZH2, also has histone H3 methylase activity and binds to an overlapping subset of genes (Margueron et al. 2008; Shen et al. 2008). EZH1 is also broadly expressed and is enriched in nonproliferative adult tissues. That said, it has been proposed that the two proteins associate with somewhat different PCR2 complexes and contribute somewhat differently to Polycomb-mediated gene repression. Our previous *in vivo* studies have shown that EZH1 and EZH2 are both expressed in skin, and both can establish the H3K27me3 histone mark at epidermal differentiation genes *in vitro* (Ezhkova et al. 2009). These collective studies point to the importance of conditionally targeting *Ezh1* *in vivo* in the presence and absence of *Ezh2* in order to uncover the

role of EZH1 specifically and H3K27me3 generally in the normal homeostasis of adult mammalian tissues.

We have now done so, focusing on the skin epidermis and its prominent but dispensable appendage, the hair follicle (HF), which features its own appendage, the sebaceous gland (SG). HFs are particularly well-suited for exploring the importance of epigenetic chromatin modifiers, since they undergo cyclical bouts of degeneration (catagen), rest (telogen), and regeneration (anagen) that necessitate a substantial reservoir of SCs. HF-SCs reside in each HF in a region called the bulge, located just below the SG in the outer root sheath (ORS) (Supplemental Fig. 1). When activated at the start of the hair growth phase (anagen), HF-SCs regenerate the cycling portion of the HF, below the bulge. They produce a trail of ORS cells that extends from the bulge to the base (bulb) of the HF, where the ORS forms a large pool of transit-amplifying (TA) matrix cells. Matrix cells proliferate rapidly but transiently, soon opting for one of several programs of upward differentiation that constitute the hair (medulla, cortex, and cuticle), its surrounding channel (the inner root sheath [IRS]), and a companion layer that is sandwiched in between the IRS and ORS (Blanpain and Fuchs 2009; Schneider et al. 2009). While their normal role is to fuel the hair cycle, HF-SCs can be activated to re-epithelialize epidermis and SGs in response to wounding (Tumbar et al. 2004; Levy et al. 2005, 2007; Horsley et al. 2006; Ito et al. 2007).

In the present study, we show that loss of either EZH1 or EZH2 alone is without apparent consequence to skin integrity. In contrast, loss of both of these histone methylases abolishes the H3K27me3 mark and severely compromises HF formation and maintenance. Surprisingly, while proliferation and cell survival are markedly impaired in both the HF-SC compartment and the TA progenitors that fuel hair growth, the epidermis is hyperproliferative and survives long-term engraftment. In contrast, in culture, neither HF nor epidermal progenitors survive. These differences afford a unique opportunity to explore the diverse consequences of quantitative loss of H3K27me3 chromatin modification in three different postnatal progenitor populations *in vivo* and their different behaviors *in vitro*. In so doing, we uncovered the hitherto unrecognized existence of compensatory and tissue-specific mechanisms that can be activated in certain situations in SCs to lessen the consequences of loss of PcG modification that dramatically affect life and death decisions.

Results

The Polycomb complex is required for the HF lineage

Mice lacking EZH1 were viable, fertile, and healthy, and will be reported elsewhere. Similarly, although conditional targeting of *Ezh2* in mouse skin accelerated epidermal formation during embryogenesis (Ezhkova et al. 2009), postnatally, they too were healthy, fertile, and viable, and displayed a normal hair coat. Additionally, each follicle was histologically normal and replete with

SGs and an anatomically well-defined niche, or bulge, of SCs (Supplemental Fig. 2A,B).

In striking contrast, mice lacking both EZH1 and EZH2 in their skin were born alive, but were unable to eat, lacked milk spots, and died within 24 h after birth (Supplemental Fig. 2C). Immunofluorescence microscopy revealed a complete loss of H3K27me3 specifically in the double-knockout epithelium but not the (*K14-Cre*-negative) dermis (Fig. 1A). Singly targeted skin epithelium was still positive for the chromatin mark (Supplemental Fig. 2D), demonstrating that EZH1 and EZH2 function redundantly in establishing this epigenetic chromatin mark in skin cells.

The skin of newborn animals doubly targeted for *Ezh1* and *Ezh2* appeared normal in morphology and in their expression of differentiation markers (Supplemental Fig. 2E,F). In addition, these animals were refractory to blue dye adsorption and dehydration (body weight) assays,

substantiating the efficacy of their skin as a barrier (Supplemental Fig. 2G,H). The early postnatal lethality in these mice was therefore most likely attributable to the activity of the *K14* promoter in oral and some other internal stratified epithelia.

HF and SGs normally continue to mature during the first week of postnatal life. To analyze whether these processes were affected by loss of EZH1 and EZH2, we grafted postnatal day 0 (P0) skins onto the backs of immunocompromised *Nude* mice (Fig. 1B). Typically, this results in a developmental delay of ~1 wk. Within 14 d post-grafting (P14), *Ezh1/2* double-knockout grafts were completely hairless, in striking contrast to their wild-type littermate grafts (Fig. 1C). As expected, immunolabeling for H3K27me3 was positive for donor dermis but not epithelium. Fluorescence quantifications of these images from *Ezh1/2* double-knockout skin revealed that the nuclear levels of H3K27me3 in the epithelium were

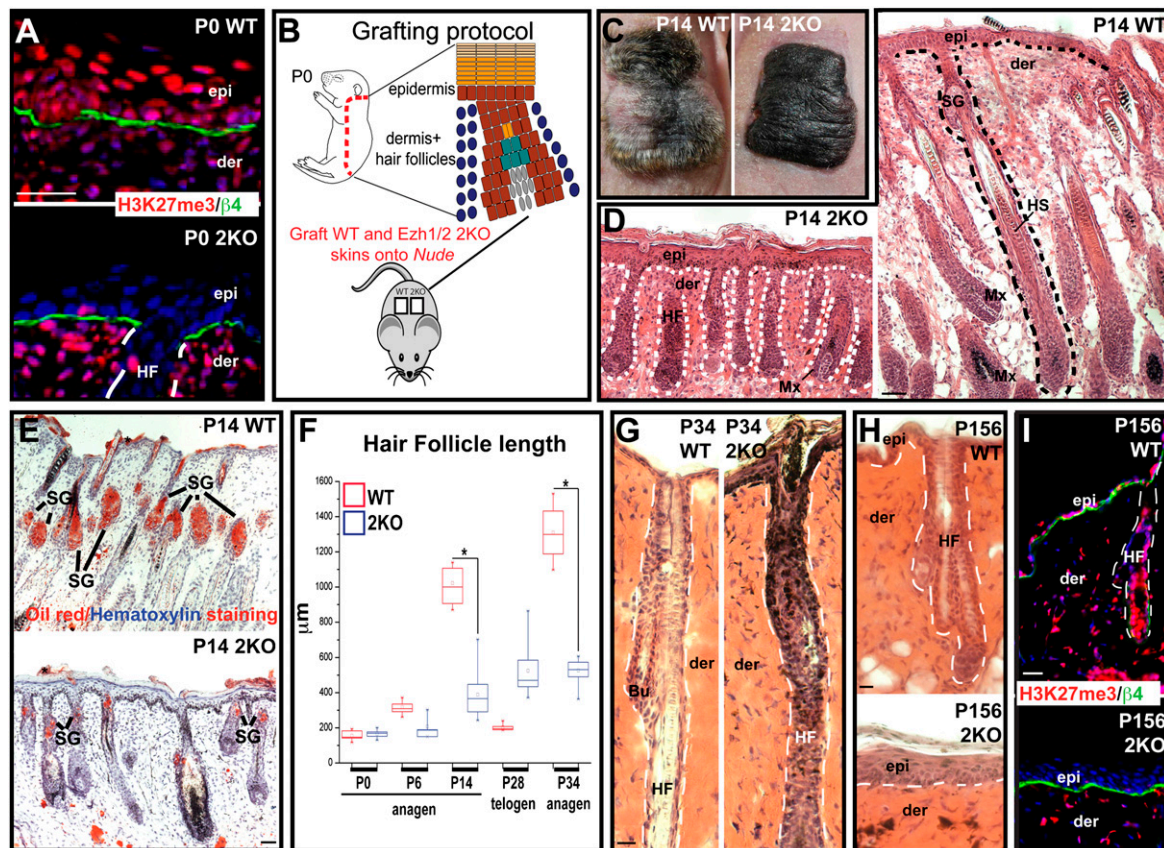


Figure 1. Arrested morphogenesis and progressive degeneration of HF and SGs lacking EZH1 and EZH2. (A) Immunofluorescence confirms the absence of H3K27me3 in P0 *Ezh1/2* double-knockout (2KO) skin epithelium. Tissue sections are counterstained for $\beta 4$ integrin (green) and chromatin (DAPI, blue). (Epi) Epidermis; (der) dermis. (B) Schematic of full-thickness grafting protocol (Kaufman et al. 2003) used to examine postnatal consequences of *Ezh1/2* ablation. (C) Absence of surface hair in double-knockout versus wild-type (WT) skin grafts. (D) Histological analysis reveals that HF of double-knockout grafts are short, and lack hair shafts (HS). (Mx) Matrix. (E) Oil-red-O stains lipids and confirms impaired SG formation in *Ezh1/2* double-knockout skins. (F) Quantification of HF lengths at times and hair cycle stages indicated. Note that double-knockout HF arrest in the first growth phase of the hair cycle. (G) The old hair and surrounding bulge (Bu) SC compartment are evident in wild-type but not double-knockout HF by P34. (H) P156 grafts reveal that wild-type HF have undergone two hair cycles, but double-knockout skin has lost all HF. Note hyperthickening of epidermis in double-knockout skin. (I) Immunofluorescence confirming that P156 double-knockout epidermis lacks H3K27me3. Bars: A, G-I, 30 µm; D, E, 90 µm.

~1000-fold less than those of dermal cells and were not distinguishable from background levels (Supplemental Fig. 3A). These data confirmed that the *Ezh1/2* double-knockout donor epithelial cells had survived and were responsible for the epidermis and HF s seen within each of the grafts (Supplemental Fig. 3A).

Histological analysis revealed marked abnormalities within double-knockout skin epithelium. At the base of each follicle, a bulb of relatively undifferentiated matrix cells still encased the cluster of dermal papilla cells in double-knockout HF s. However, HF s were stunted and appeared to lack both a mature hair shaft and also SG s, which in wild-type skin were readily visible by Oil-red-O staining for lipids (Fig. 1D,E). A paucity of sebocytes was further revealed by Ppar γ immunostaining (Supplemental Fig. 3B). Together, these data indicate a severe defect in the production of mature structures within the HF lineage of double-knockout mice.

To determine whether skin morphogenesis in *Ezh1/2* conditionally null mice was simply delayed or had arrested, we examined grafts at later time points. By P34, HF s of wild-type engrafted skins had already completed the first hair cycle and were into the next growth phase. In striking contrast, *Ezh1/2* conditional knockout follicles from the first hair cycle had arrested at an immature state, with no visible signs of hair shaft or SG formation (Fig. 1F,G; Supplemental Fig. 3C,D). As time progressed, HF morphology became increasingly perturbed, and signs of degeneration were evident (Supplemental Fig. 3E). By P156, double-knockout grafts almost completely lacked HF s (Fig. 1H). Surprisingly, however, the epidermis was intact, and immunostaining confirmed that it was still null for H3K27me3 (Fig. 1I).

Loss of EZH1/2 leads to neither changes in cell fate nor blocks in differentiation

In cultured ESC s, the Polycomb complex has been shown to repress key transcriptional regulators that control SC differentiation to different developmental lineages (Boyer et al. 2006; Lee et al. 2006). Moreover, upon retinoic acid induction, PcG-defective ESC s fail to suppress pluripotency genes and execute neuronal differentiation (Pasini et al. 2007, 2010). Thus, to dissect the biological processes that led to the impairment in HF formation and maintenance, we first verified by chromatin immunoprecipitation (ChIP) and Solexa deep-sequencing (ChIP-seq) analysis that HF-SC s are similar to ESC s in targeting multiple developmental lineage genes by the H3K27me3 histone mark (W-H Lien and E Fuchs, in prep.). We then focused on analyzing whether HF cells maintain their cell fate and are able to undergo differentiation in the absence of H3K27me3.

At P14, both wild-type and double-knockout follicles showed normal expression of K14's partner, K5, in the ORS and K6 in the companion layer (Supplemental Fig. 4A). Similarly, antibodies specific for trichohyalin (AE15) detected an IRS, and those specific for hair keratins (AE13) detected a cortical layer in both wild-type and double-knockout follicles (Supplemental Fig. 4B,C). That

said, the medulla at the center of the hair shaft appeared to be missing in the double-knockout follicles, as judged by a lack of anti-K6 and AE15 labeling and the lack of any cells central to the AE13-positive hair shaft cortex. Ultrastructural analysis confirmed these findings (Supplemental Fig. 4D). Like the cortex, IRS, and companion layer, the medulla arises from differentiation of the matrix. However, since the medulla is the last of the matrix lineages to emerge during normal HF morphogenesis, it seems more likely that its absence reflected a failure to progress through morphogenesis rather than a differentiation defect per se. We revisit this issue again later.

For the epidermis and hair channel orifice (infundibulum), both early and late differentiation markers were localized normally (Supplemental Fig. 4E,F). The absence of cell fate alterations differed from cultured ESC s but was in good agreement with observations on embryonic basal epidermal cells lacking H3K27me3 (Ezhkova et al. 2009). However, in contrast to *Ezh2* conditional knockout embryonic epidermis, *Ezh1/2* double-knockout postnatal skin displayed no signs of accelerated development/differentiation. Rather, postnatal epidermal homeostasis seemed relatively normal, while HF tissue production was arrested.

SC s are specified in double-knockout skin

The block in SG development and arrest in HF morphogenesis observed in our *K14-Cre*-mediated conditional ablation of *Ezh1/Ezh2* bore a marked resemblance to *K14-Cre*-mediated conditional ablation of *Sox9* (Nowak et al. 2008). These events in tissue development are dependent on slow-cycling, *Sox9*-expressing bulge SC s that are specified early during development and are located in the upper portion of the ORS (Nowak et al. 2008; Vidal et al. 2008). We therefore wondered whether the *Ezh1/Ezh2* double-knockout phenotype might originate from a failure to form this early SC compartment.

To test this hypothesis, we immunolabeled P0 skins for *Sox9*, *Lhx2*, and *Nfatc1*, three key transcription factors of early HF-SC s. In contrast to *Sox9* targeted skin, *Ezh1/Ezh2* double-knockout mice faithfully expressed all three of these factors, suggesting that HF-SC s had been specified (Fig. 2A; Supplemental Fig. 5). Since HF morphogenesis occurs in waves, some follicles were more mature than others at P0, but overall patterns were comparable between wild type and double-knockout. Moreover, even in P14 engrafted double-knockout tissue when HF and SG formation was clearly arrested, the early bulge cells appeared to be present in normal locations and numbers (Fig. 2B,C). During embryogenesis, SG progenitors are derived from *Sox9*-expressing cells (Nowak et al. 2008). To determine whether this lineage progression takes place in the absence of H3K27me3, we immunolabeled for *Blimp1*, a critical transcriptional repressor of sebocyte progenitors (Horsley et al. 2006). Again, even at P14 when SG development was clearly perturbed, *Blimp1*-expressing sebocyte progenitors appeared to be present in the ORS in the vicinity of where SG s should have developed (Fig. 2D).

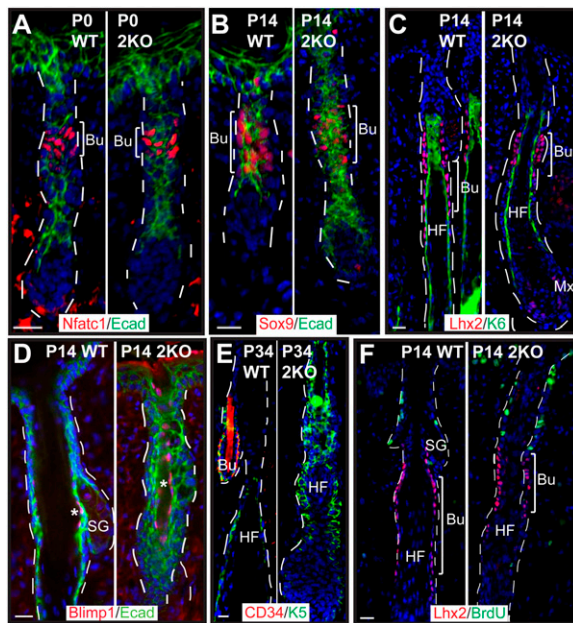


Figure 2. Cells expressing HF-SC and SG-SC markers are still present in *Ezh1/2* double-knockout skin. (A–E) Immunofluorescence microscopy of sections from P0 (A), P14 (B–D), or P34 (E) skin grafts analyzed for temporal and spatial expression of SC markers. Color-coding is according to the secondary antibodies used. *Blimp1* is a marker of SG-SCs; *Nfatc1*, *Lhx2*, *Sox9*, and *CD34* are HF-SC markers. (F) A short (4-h) BrdU pulse followed by immunofluorescence analysis shows that, similar to wild type, none of *Lhx2*⁺ SCs are BrdU-labeled. In contrast, the cells above the bulge are hyperproliferative in double-knockout compared with wild-type skin. Bar, 30 μ m.

While SCs appeared to be properly specified in the absence of EZH1 and EZH2, some abnormalities in SC markers were discovered. Notable was CD34, which was present in the HF bulge region of engrafted skins from wild-type but not double-knockout mice (Fig. 2E). Since CD34 is a marker of only postnatal and not neonatal HF-SCs (Trempe et al. 2003; Blanpain et al. 2004; Nowak et al. 2008), this appeared to be another reflection of an early developmental arrest of postnatal double-knockout HF-SCs and their inability to progress to adulthood.

To further explore the properties of double-knockout HF-SCs, we addressed whether they are quiescent, a feature of both neonatal and adult HF-SCs (Cotsarelis et al. 1990; Tumber et al. 2004; Nowak et al. 2008). A short (5- to 6-h) BrdU pulse was administered to wild-type and *Ezh1/Ezh2* double-knockout mice (Fig. 2F). Counterlabeling for SC markers further showed that, typical of wild-type follicles in the middle of their growth phase, double-knockout bulge SCs and their early upper ORS progeny remained relatively quiescent. Together, these data indicated that the arrested HF and SG development observed in double-knockout skin was not likely due to a lack of SCs per se, or their ability to maintain the undifferentiated and quiescent features of their wild-type counterparts. However, the HF-SCs of double-knockout

skin did not express the full complement of mature HF-SC markers, nor did they appear to generate tissue at the rate of their wild-type counterparts.

Without EZH1/EZH2, the HF-SC lineage exhibits proliferation deficits while the epidermal SC lineage shows signs of hyperproliferation

Interestingly, proliferative activity in the lower portion of double-knockout HF-SCs showed a striking reduction compared with their wild-type counterparts. Indeed, double-knockout matrix cells appeared to have reduced numbers of BrdU⁺ cells compared with their wild-type counterparts (Fig. 3A,B). The double-knockout follicle matrix was also noticeably small (Fig. 3A,C). Analysis of the proliferative marker Ki67 (S + M-phase cells) confirmed the markedly reduced proliferation within the double-knockout matrix compartment (data not shown). Together these data indicate that both the size and the proliferation rates within the TA compartment are defective when EZH1 and EZH2 are missing.

The small matrix could be due to a defect in their ability to proliferate. However, it also could be a sign of a compromised ability of HF-SCs to fuel tissue regeneration during morphogenesis. To address this question, we focused on the region of the follicle ORS between the HF-SCs and matrix. In wild-type HF-SCs, cells in the upper zone of this ORS segment maintain their stemness and cycle infrequently, while cells in the lower ORS proliferate more rapidly. BrdU pulse experiments on wild-type and double-knockout mice showed little if any difference in BrdU incorporation in the upper zone of the ORS below the bulge; however, the lower zone showed a marked decline in BrdU⁺-labeled cells when EZH1 and EZH2 were missing (Fig. 3D,E). Taken together, these findings suggest that double-knockout HF-SCs do not produce sufficient ORS cells to fuel matrix cell production.

In striking contrast to the HF-SC lineage, proliferative activities within the infundibulum of the HF and the basal layer of double-knockout interfollicular epidermis were actually accelerated relative to wild-type control skin (Fig. 3F–I). Moreover, although P14 double-knockout epidermis showed considerably more BrdU⁺ basal cells than at later time points, even at P73, double-knockout basal cells were still more actively cycling than their wild-type counterparts (Fig. 3H,I). Taken together, these findings revealed marked differences in proliferative activities within the epidermal versus HF progenitors of double-knockout skin.

A priori, epidermal hyperproliferation can be reflective of an inflammatory response, rather than an intrinsic feature of the keratinocyte. In this case, however, we did not observe signs of inflammation, as judged by immunodetection for T lymphocytes, granulocytes, and macrophages (Supplemental Fig. 6A). Moreover, even after treating with dexamethasone as an immunosuppressor, double-knockout skin grafts continued to display signs of epidermal hyperproliferation (Supplemental Fig. 6B–D). Thus, neither sustained survival of the double-knockout epidermis nor corresponding loss of HF-SCs/SGs appeared to rely on an inflammatory response.

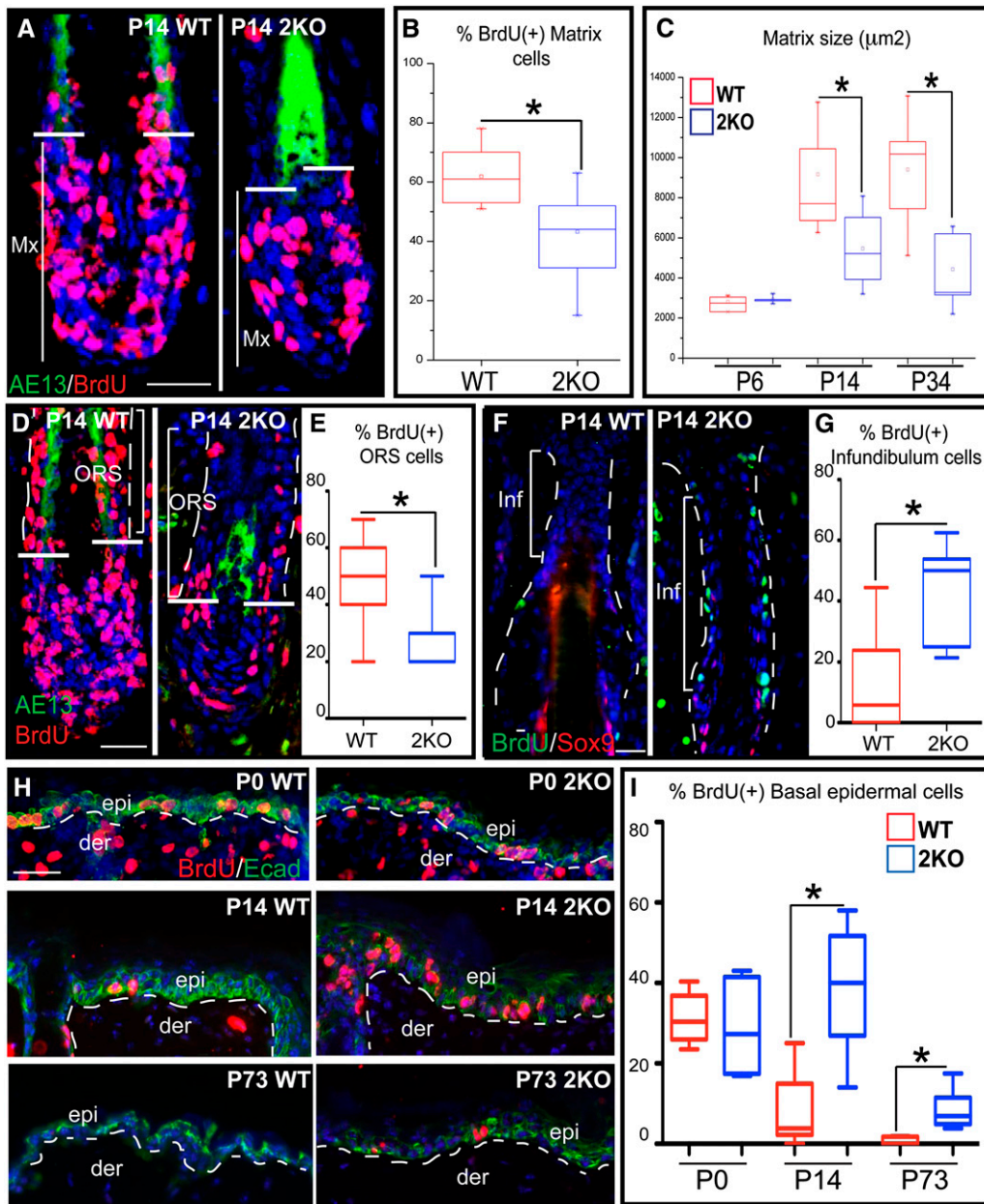


Figure 3. Loss of EZH1/2 results in reduced proliferation of HF ORS and matrix, but hyperproliferation in infundibulum and epidermis. (A–E) A short (4-h) BrdU pulse was administered to engrafted mice prior to processing the engrafted tissue for anti-BrdU and hair keratin (AE13) immunofluorescence microscopy and quantitative analyses. Note reduction in proliferation in the matrix (Mx), hair shaft precursors (cells above horizontal bars and internal to or including AE13⁺ layer) and ORS (cells above horizontal bars and external to and excluding AE13⁺ layer) in double-knockout (2KO) versus wild-type (WT) skins. Note also that overall matrix size of double-knockout HFs was normal at P6, but markedly diminished by P14 and P34 post-enugraftment. (F–I) Similar analyses as in A–E, except on double-knockout infundibulum and interfollicular epidermis. Note hyperproliferation in both compartments by P14. By P73, double-knockout grafts still show more proliferation than wild type, but overall proliferative levels in the epidermis decline with age. Bar, 30 μm.

Ezh1/2 double-knockout HF-SCs are defective in proliferation even in response to stimuli

HF-SCs are known to contribute to epidermal regeneration in response to injury (Levy et al. 2005, 2007; Nowak et al. 2008). To test whether HF-SCs lacking EZH1 and EZH2 are compromised in their tissue-regenerative ca-

capacity, we performed split-thickness grafts, in which skin epidermis from male P0 mice is first enzymatically removed from underlying dermis, and then remaining dermis/HFs are grafted onto the backs of female *Nude* mice recipients (Fig. 4A). To repair the wound, male HF-SCs proliferate, migrate, and repair the surface epithelium. They also compete with *Nude* epidermal cells that

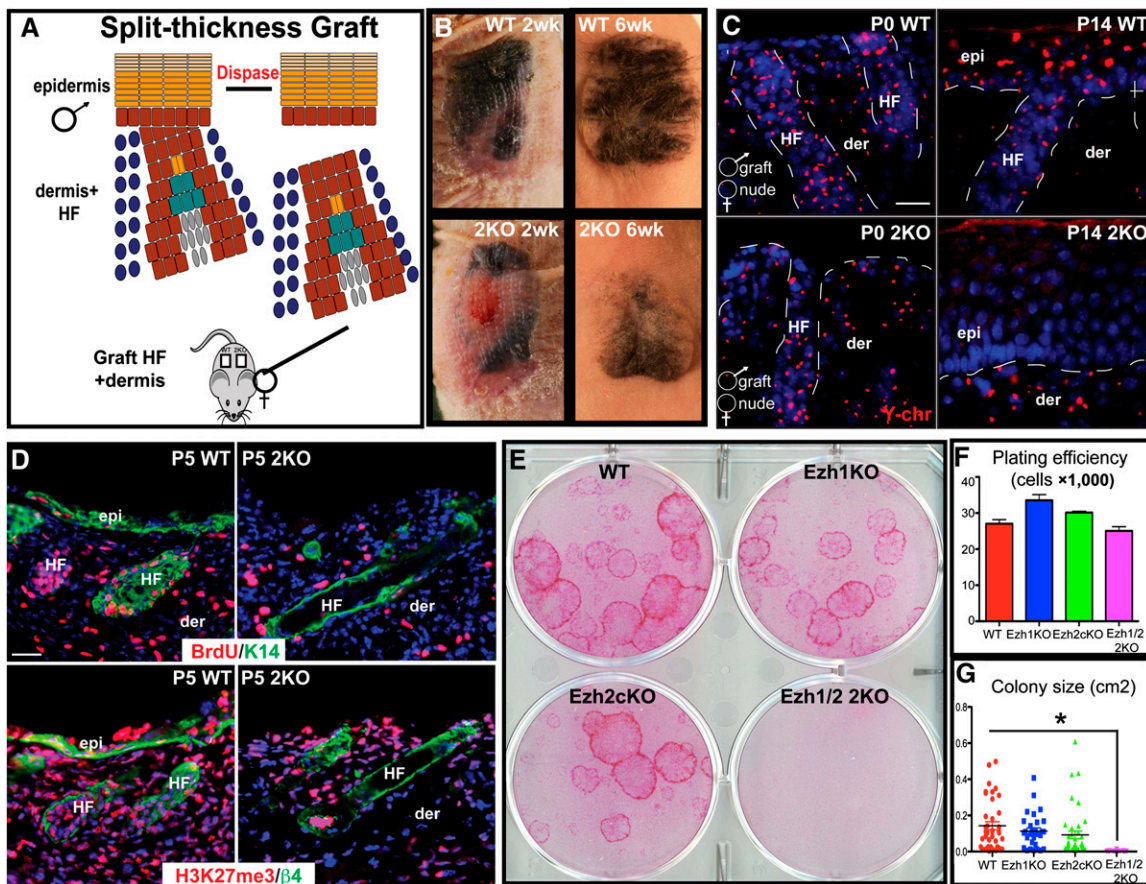


Figure 4. Double-knockout HF are defective in proliferation even upon wound-induced stimulation. (A) Schematic of split-thickness grafting protocol. The ability of HF cells to migrate out and re-epithelialize the epidermis is largely dependent on functional bulge SCs, although wounds will eventually close by *Nude* mouse epidermal migration (Nowak et al. 2008). Male dermis + HF are engrafted onto female *Nude* mice to distinguish the two events by Y-chromosome in situ hybridization. (B) Six weeks after engraftment, double-knockout split thickness grafts finally close their wounds, a feat accomplished by their wild-type counterparts in 2 wk. (C) At P0, epidermis is completely missing in split-thickness grafts. By P14, re-epithelialization of wild-type grafts is accomplished largely by HF migration (Y-chr⁺). In double-knockout grafts, re-epithelialization, still in progress, is exclusively by *Nude* host-derived epidermal migration. (D) A short BrdU pulse administered 5 d post-engraftment shows lack of a proliferative response by the H3K27me3-deficient HF of double-knockout skin. (E–G) Double-knockout HF progenitors are unable to proliferate in vitro. (E) Rhodamine B staining of primary mouse HF cultures after 3 wk in enriched media. Note that only doubly targeted cells fail to form visible colonies. Quantifications show that plating efficiencies are comparable but colonies simply fail to grow in the absence of H3K27me3. Bar, 30 μ m.

migrate from outside of the graft to close the wound (Nowak et al. 2008).

Two weeks after performing split-thickness engraftments, wild-type grafts had completely re-epithelialized the epidermis, and even showed signs of growing a hair coat (Fig. 4B). On the other hand, double-knockout split-thickness grafts still displayed a bare epidermis in the middle of the graft, indicating that double-knockout SCs were defective in their ability to re-epithelialize the surface skin. Eventually, the wounds were closed and, by 6 wk after engraftment, the skin surface was repaired (Fig. 4B).

To ascertain whether wound closure in double-knockout split-thickness grafts was a consequence of HF-SCs or *Nude* epidermal migration, we used Y-chromosome fluorescence in situ hybridization (Y-FISH). Y-FISH revealed that, at P14 and P42, the interfollicular epidermis

in double-knockout split-thickness grafts was host-derived, as no Y labeling was observed (Fig. 4C; data not shown). This was confirmed by H3K27me3 immunofluorescence (Supplemental Fig. 7A). In contrast, although reconstituted epidermis in wild-type split-thickness grafts was positive for H3K27me3, it was also positive for Y-FISH, indicating that the cells originated from HF (Fig. 4C).

Consistent with the defect in the ability of double-knockout HF-SCs to participate in wound repair was a defect in their proliferative response. Thus, in contrast to wild-type HF, which showed appreciable incorporation of BrdU in a short (4-h) pulse 5 d following engraftment, double-knockout HF exhibited little if any BrdU incorporation (Fig. 4D). These data indicated that HF from double-knockout skin are defective in proliferating and regenerating tissue in response to injury.

To further investigate the proliferative ability of double-knockout HF cells, we turned to *in vitro* studies. When plated in culture, wild-type HF cells develop into large (>2-mm) colonies or holoclones, thought to derive from individual SCs (Barrandon and Green 1987). HF cells from either *Ezh1* knockout or *Ezh2* conditional knockout follicles formed holoclones with efficiencies comparable with their wild-type counterparts (Fig. 4E–G). In striking contrast, even after >4 wk in culture, *Ezh1/Ezh2* double-knockout HF cells showed no signs of forming visible colonies. This difference was not rooted in the ability of these cells to adhere, which was similar to wild type (Fig. 4F). Rather, it appeared that, in the absence of EZH1 and EZH2, HF cells were defective in proliferation.

Since *Ezh1/Ezh2*-null epidermis was hyperproliferative *in vivo*, we anticipated that epidermal keratinocytes *in vitro* would be similarly proliferative. Unexpectedly, however, *Ezh1/2*-null epidermal and HF keratinocytes behaved analogously *in vitro*, with no large colonies visible after 4 wk in culture (Supplemental Fig. 7B–D). This result revealed a striking difference in behavior of *Ezh1/Ezh2*-null epidermal keratinocytes *in vivo* and *in vitro*, and points to the existence of some mechanism that enables H3K27me3-deficient epidermal cells to survive in the context of tissue.

Increased apoptosis in double-knockout HF cells

Tissue homeostasis involves a tight balance between proliferation, differentiation, and apoptosis. In the HF, apoptosis is normally confined to the destructive phase (catagen), where the matrix compartment degenerates. However, in double-knockout skin, activated caspase 3⁺ cells were detected in HFs and at a stage where their wild-type counterparts were in the active growth phase (Supplemental Fig. 8A). Quantifications of immunolabeling for activated caspase 3 revealed an approximately threefold overall increase in apoptotic cells in double-knockout versus wild-type HFs, which was confirmed by ultrastructural analyses (Supplemental Fig. 8B,C).

In contrast, we saw little or no evidence for apoptosis in the epidermis of our engrafted animals at the level of either immunofluorescence (Supplemental Fig. 8D) or ultrastructure (data not shown). Thus, both proliferation and cell survival appeared intact in double-knockout epidermis, and in this way differed from HFs.

Complete loss of H3K27me3 in different proliferative compartments in skin results in the activation of a common 'PcG signature' list of genes

To begin to explore how H3K27me3 loss of function can lead to such a diversity of tissue imbalances within the skin, we performed microarray analysis on mRNAs isolated from fluorescence-activated cell-sorted (FACS) populations of the ORS (including bulge), matrix, and basal layer epidermis (Supplemental Table 1). The purity of sorted populations was verified by analysis of expression of nonskin genes (Supplemental Table 2; Supplemental Fig. 9A). In wild-type mice, these cell populations

display quite distinct programs of gene expression, extending to the major lineage-specific transcription factors involved (Blanpain and Fuchs 2009). In contrast, when EZH1/2 were missing, ORS, matrix and epidermal mRNAs displayed many shared probe sets called as present and up-regulated by twofold or more (Fig. 5A). These findings suggested that a common subset of genes is regulated by the H3K27me3 PcG mark in different populations of skin cell progenitors, and when this chromatin modification is erased, their transcriptional repression is diminished.

The common subset of up-regulated genes represented only 30% of the mouse genes that scored by ChIP-seq as being decorated by H3K27me3 marks in purified populations of postnatal skin progenitors (Fig. 5B; data not shown). Hierarchical clustering analysis revealed that genes up-regulated in double-knockout ORS do not cluster with genes expressed in either wild-type matrix or wild-type basal epidermal cells. These data were consistent with the biology, and showed that, upon EZH1/2 loss, ORS/HF-SC progenitors do not globally precociously/ectopically express other skin lineage genes. Importantly, genes that are normally induced as wild-type HF-SCs transition to matrix cells did not appear to be preferentially repressed by H3K27me3 (Fig. 5C). Taken together, these results suggest that, in contrast to embryonic epidermis (Ezhkova et al. 2009), H3K27me3 does not govern repression of skin lineage-specific programs in undifferentiated postnatal skin progenitors. Instead, EZH1/2 appear to repress a common subset of genes controlling other features of tissue biology.

To gain further insights into PcG's functions, we examined the specific ORS genes whose expression is affected by loss of EZH1/EZH2. By using a functional gene annotation tool (Huang et al. 2009), probe sets were subdivided into categories. By comparing expression trends of genes within categories, we learned that key transcriptional regulators of nonskin cell lineages were featured prominently in the signature, along with the *Ink4a/Arf* and *Ink4b* genes, which regulate the G1/S transition of the cell cycle and control of apoptosis (Fig. 5D). These results were strikingly similar to the genes up-regulated upon loss of EZH2 in cultured human ESCs (Boyer et al. 2006), but again differed from embryonic epidermis, where progenitors do not activate nonskin genes (Ezhkova et al. 2009).

To probe further into the mechanisms involved, we compared the overall expression levels of nonskin genes in their native lineages with the levels of ectopic gene derepression achieved by loss of EZH1/EZH2 in skin. As shown in Figure 5E, the levels of nonskin gene activation in *Ezh1/Ezh2*-null matrix, epidermal, and ORS skin progenitors were considerably lower than those achieved by the native lineages (+Ctrl). These results underscore the existence of additional mechanisms, presumably tissue-specific factors, which govern the optimal expression of these genes. Moreover, they extend significantly our prior observations from basal epidermal cells of *Ezh2* conditional knockout embryos, which showed that mere removal of the H3K27me3 mark does not guarantee that a locus relieved of PcG modifications will be transcribed (Ezhkova et al. 2009).

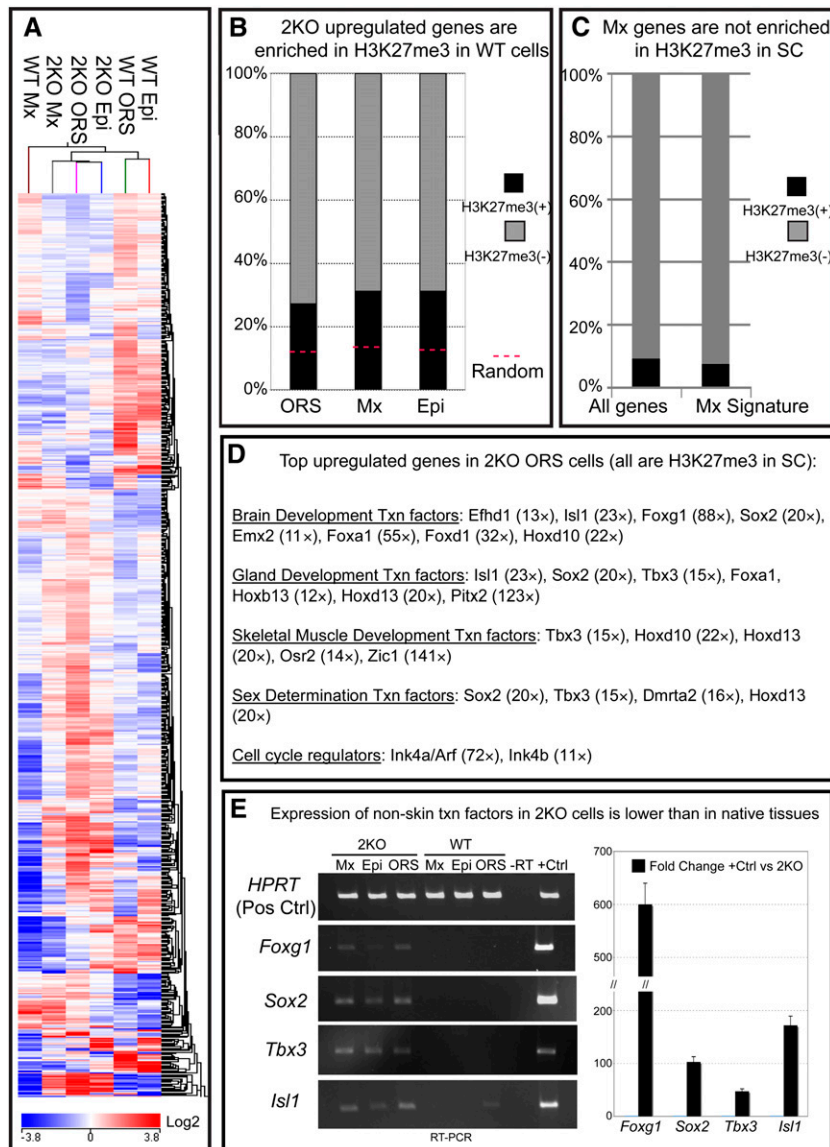


Figure 5. Ablation of *Ezh1/2* leads to the up-regulation of a common subset of genes in three different skin progenitors irrespective of their lineage and response to deregulation of PcG-mediated repression. (A) Heat map and clustering analyses reveal that many genes differentially expressed in double-knockout progenitors of ORS, matrix (Mx), and epidermis (Epi) cocluster together. Notably, genes up-regulated in double-knockout ORS progenitors do not cocluster with wild-type matrix or wild-type epidermis cells, indicating that double-knockout progenitors are not induced to progress toward HF (matrix) or epidermal lineages. (B) The *Ezh1/2* up-regulated genes of each skin progenitor type was compared against ChIP-seq data mapping H3K27me3 (PcG-repressive) and H3K79me2 (active transcription) marks in the chromatin of postnatal bulge SCs, matrix TA cells, or epidermal basal progenitors. Whole-scale comparative analysis reveals that one-third of genes up-regulated in double-knockout ORS, matrix, or epidermis are targeted by H3K27me3 repression in wild-type progenitors. (C) Genes that are normally activated in wild-type matrix cells are not preferentially repressed by H3K27me3 histone mark in SCs, explaining why genes controlling matrix lineage determination are not preferentially up-regulated when H3K27me3 marks are removed from ORS stem cell progenitors. (D) Top up-regulated genes in double-knockout ORS cells that are regulated by H3K27me3 in wild-type ORS bulge SCs. Fold up-regulation is given in parentheses. (E) Real-time PCR reveals that ectopic activation of genes encoding nonskin lineage transcription factors in all three skin progenitors is significantly lower compared with their levels within native tissues (+Ctrl). Quantifications are shown at right.

EZH1 and *EZH2* repress *Ink4b/Ink4a/Arf* genes

Ink4a and *Ink4b* encode the p16 and p15 inhibitors of the G1/S phase of the cell cycle, and *Arf* encodes the p19 inhibitor of the p53 suppressor MDM2 (Sherr and Roberts 2004). The perturbations in proliferation and apoptosis seen in both the HF-SC and TA cell compartments suggested that the >70-fold increase in *Ink4a/Arf* and >10-fold increase in *Ink4b* gene transcription are physiologically relevant. To test this hypothesis, we first conducted ChIP-seq analyses on HF-SCs and matrix and basal epidermal progenitors. As shown in Figure 6A, the *Ink4a/Arf* and *Ink4b* genes are replete with H3K27me3 chromatin modifications in all three progenitor populations. Conversely, these genes lacked H3K79me2, a modification that is normally present throughout the chromatin of actively transcribed genes (Fig. 6A; Barski et al. 2007).

We next used real time PCR (RT-PCR) to examine the relative transcript levels from these loci in the three progenitor populations purified from wild-type and *Ezh1/2* double-knockout skins (Fig. 6B). Both the ORS/bulge and matrix progenitors displayed particularly dramatic transcriptional changes at the *Ink4a/Arf* locus. Interestingly, however, and also likely relevant, differences were not nearly so great in the epidermis, most notably for *Ink4a* (Fig. 6B).

Immunofluorescence microscopy reflected these transcriptional differences at the protein level (Fig. 6C,D). Both p16 and p19 proteins were localized to the nucleus of double-knockout HF cells. Particularly for p16, immunolabeling was considerably stronger in HFs than in interfollicular epidermis or infundibulum (Fig. 6C). No signal was observed in *Ink4a/Arf* double-knockout skin, validating the efficacy of the antibodies. Quantifications corroborated the representative images shown (Fig. 6E,F;

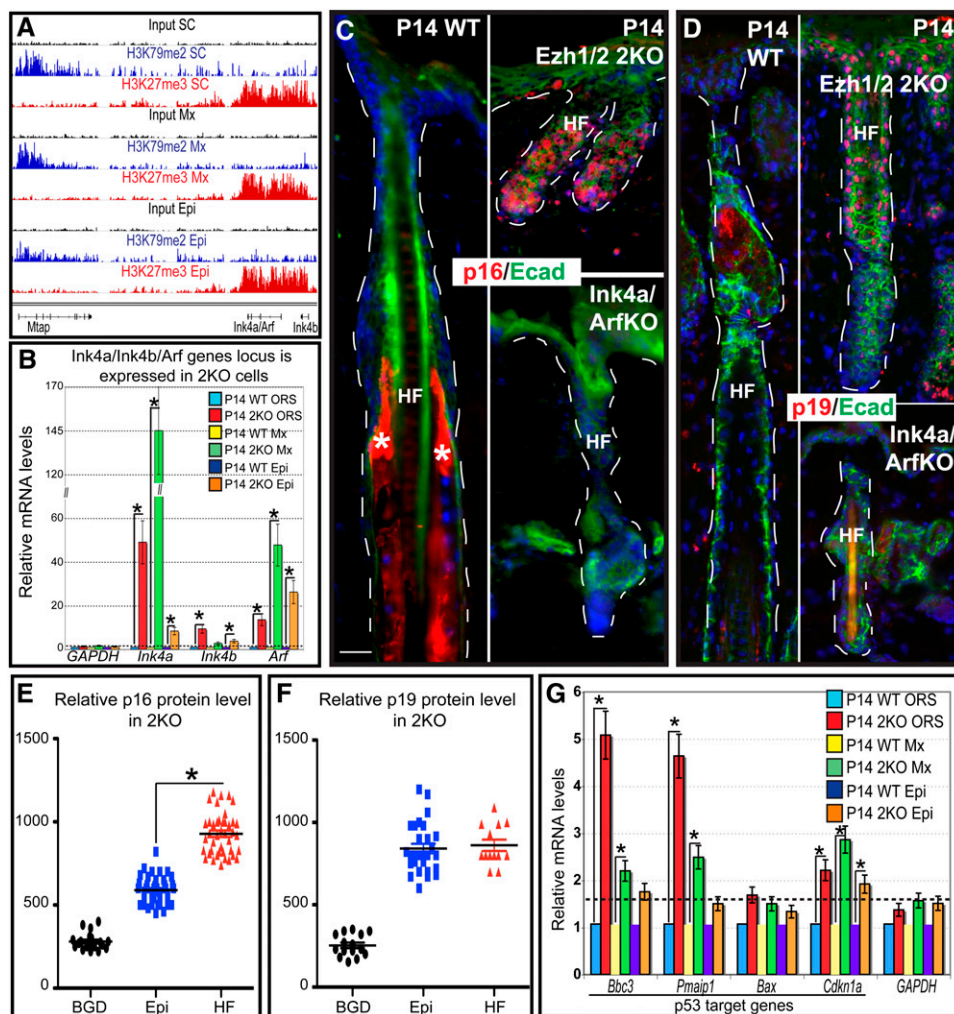


Figure 6. The *Ink4b/Ink4a/Arf* gene locus is targeted by EZH1/2-dependent H3K27me3 in skin progenitors, but activation levels upon *Ezh1/2* ablation differ markedly among skin progenitor populations. (A) ChIP-seq data reveal that the *Ink4b/Ink4a/Arf* gene locus is targeted by H3K27me3 in bulge SCs (SC)/ORS, matrix (Mx), and basal epidermal (Epi) cells. ChIP-seq for the H3K79me2 histone mark confirms that these H3K27me3-decorated genes are in a repressed state. The housekeeping gene *Mtap* is shown here as a control. (B) RT-qPCR reveals that *Ink4b*, *Ink4a*, and *Arf* genes are all up-regulated in double-knockout skin progenitors relative to their wild-type counterparts, but the levels of induction vary dramatically among progenitor populations. (C,D) Immunofluorescence confirms variation in the induction of p16 (*Ink4a*) and p19 (*Arf*) by epidermal versus HF progenitors. *Ink4a/Arf* knockout tissue was used to control for antibody specificity. Note elevated nuclear (active) p16 and p19 labeling in double-knockout progenitors, not seen in wild type. Wild type only shows cytoplasmic staining (asterisk) of terminally differentiated HF lineages. (E,F) Quantifications of relative protein levels shows that p16 is significantly lower in double-knockout epidermis versus HF, while p19 levels are comparable. (G) p19 stabilizes p53, whose transcriptional activity can be monitored by activation of its target genes: *Bbc3* (PUMA; proapoptotic protein), *Pmaip1* (NOXA; proapoptotic protein), and *Bax* and *Cdkn1a* (p21). Note that, despite comparable expression of p19 protein in double-knockout epidermis and HFs, p53 target proapoptotic genes are significantly more activated in the HF than epidermal progenitors. Bar, 30 μ m.

see the Supplemental Material for details of quantification methods).

Finally, the up-regulation of p19 should lead to p53 activation. Indeed, a number of p53 target genes were elevated in *Ezh1/2* double-knockout skin relative to controls (Fig. 6G). This was true for ORS and matrix but not interfollicular epidermis basal cells. Taken together, these findings demonstrated that loss of the H3K27me3 mark was sufficient to derepress the *Ink4b/Ink4a/Arf* locus, leading to transcriptional activation of these genes. However, they also unveiled differences in how epider-

mal and HF progenitors responded to H3K27me3 loss. Overall, the results for this locus correlated strongly with the phenotypic differences between epidermis and HFs, thereby underscoring the likely physiological relevance.

Expression of Ink4b/Ink4a/Arf genes in double-knockout HF progenitors is directly responsible for impeding their proliferative activity

To determine the extent to which the global decrease in HF proliferation was directly attributable to the aberrant

activation of *Ink4a/Arf-Ink4b* genes, we performed RNAi experiments. To accomplish this aim, HF cells were purified from P0 animals, placed into culture, and then infected with lentiviral vectors expressing GFP-tagged histone H2B and an shRNA construct targeting *Ink4b* (sh-*Ink4b*) ± *Ink4a/19* (sh-*Ink4a/Arf*) or no mRNA (sh-*Ctrl*). To assay proliferation, infected cells were plated onto fibroblast feeders, and colony formation was analyzed over time.

Two weeks after infection, wild-type or double-knockout cells expressing either sh-*Ctrl*, sh-*Ink4b*, sh-*Ink4a*, or sh-*Ink4b* + sh-*Ink4a/Arf* formed visible colonies (four or more cells) (Fig. 7C; data not shown). Expression of sh-*Ink4b* + sh-*Ink4a/Arf* did not significantly affect growth of wild-type HF cells, but the effect on double-knockout HF cells was dramatic. Surprisingly, these effects were largely due to suppression of *Ink4b*, and only a modest gain was obtained when both *Ink4a/Arf* and *Ink4b* were targeted for repression. Histological and quantitative analyses revealed that colony morphology, efficiency of colony formation, and the proliferative potential was

largely restored upon knockdown of these genes in *Ezh1/2* double-knockout keratinocytes (Fig. 7A–D). Immunofluorescence of transduced cells verified that H3K27me3 was still absent (Fig. 7E), and that the shRNAs had the expected effects on repressing their respective mRNAs (Fig. 7F). As shown in Figure 7G, suppression of the *Ink4a/Arf/Ink4b* locus did not affect the ability of progenitors to undergo calcium-induced terminal differentiation. Overall, the results emphasize the importance of PcG-mediated repression of the *Ink4a/Arf/Ink4b* locus for self-renewal and survival of HF progenitors. However, they also uncovered a new difference—the importance of *Ink4b* (p15) in vitro versus *Ink4a* (p16) in vivo—for these progenitors.

Finally, we examined the expression of the nonskin genes that we found to be repressed by PcG/H3K27me3 and ectopically activated in postnatal skin progenitors. Unexpectedly, and in contrast to postnatal skin progenitors in vivo, the cultured double-knockout keratinocytes expressing *Ink4a/Arf/Ink4b* shRNAs showed no signs of ectopic activation of nonskin genes (Fig. 7H). Although

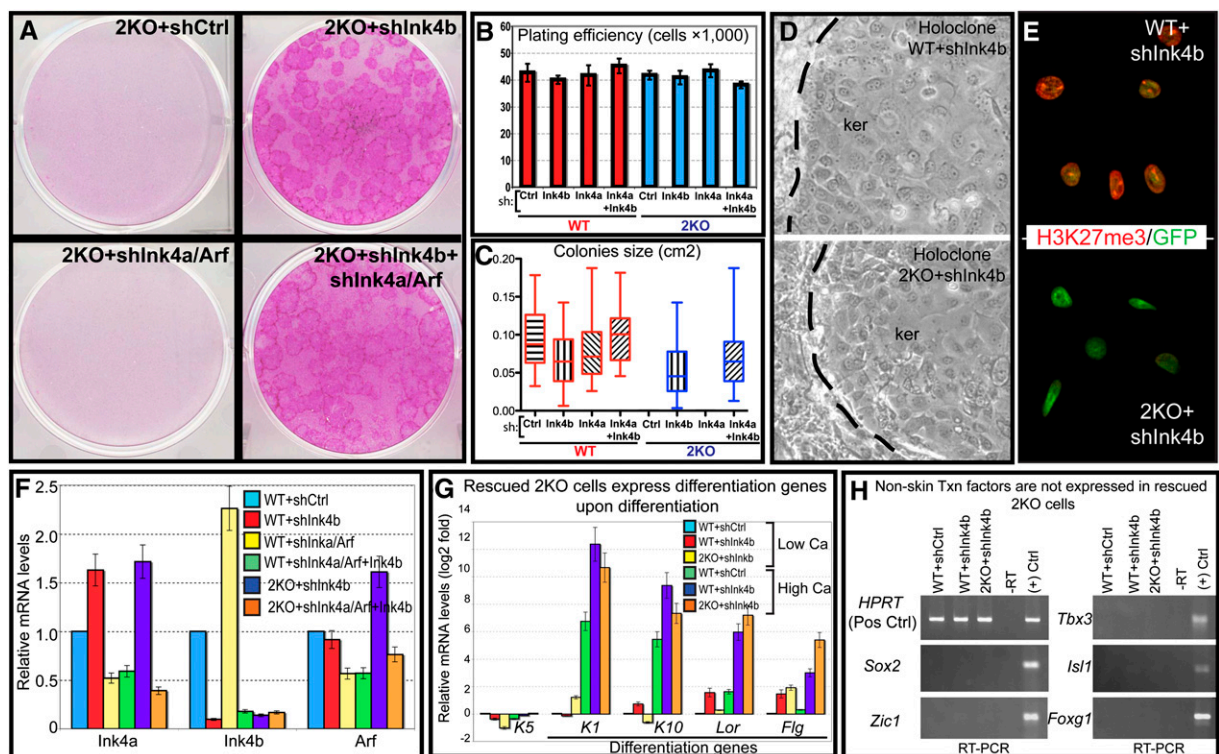


Figure 7. shRNA-mediated down-regulation of *Ink4b/Ink4a/Arf* expression restores proliferation of *Ezh1/2* double-knockout HF progenitors in vitro. (A–D) P0 wild-type and double-knockout HF cells were cultured and transduced with lentiviral expression vectors harboring shRNA hairpins that target *Ink4a/Arf* (shared region) and/or *Ink4b*. Rhodamine B staining (A) and quantification (B,C) revealed that double-knockout cells expressing control (scrambled) shRNA or shRNA targeting *Ink4a/Arf* fail to form visible colonies 4 wk after plating, in contrast to double-knockout cells expressing *Ink4b* and (optimally) *Ink4b* + *Ink4a/Arf*. Plating efficiencies (B) were comparable, but proliferation (C) and colony morphologies (D) were significantly enhanced when the locus was repressed. (E) Immunofluorescence confirms that the sh-*Ink4b* transduced (GFP⁺) double-knockout cells still lack the H3K27me3 mark in contrast to transduced wild-type cells. (F) Efficiencies of RNAi knockdown of *Ink4b* and *Ink4a/Arf* genes as analyzed by RT-qPCR on FACS-isolated populations 4 wk after transduction. (G) Double-knockout + sh-*Ink4b* cells are able to induce terminal differentiation genes keratin 1 (K1), keratin 10 (K10), *loricrin* (Lor), and *filaggrin* (Flg) upon a shift from low to high calcium. Analysis is by RT-qPCR. (H) Genes encoding transcription factors of nonskin lineages are not expressed in cultured HF progenitors that can grow following rescue of the *Ink4a/Arf/Ink4b* locus.

double-knockout keratinocytes do not grow in culture without suppressing the *Ink4a/Arf/Ink4b* locus, the required repression of these genes in the absence of PcG was not likely a consequence of the suppression of this locus. Rather, our findings show that, whereas nonskin PcG-regulated genes can be induced—in some cases, >100-fold—in vivo when EZH1 and EZH2 are missing, they can also be repressed in a PcG-independent fashion.

Discussion

Although in vitro EZH1 and EZH2 have been shown to be functionally redundant (Margueron et al. 2008; Shen et al. 2008; Ezhkova et al. 2009), it has been ambiguous as to whether this is the case in the context of tissue development and homeostasis. Since H3K27me3 is quantitatively abolished in skin progenitors only upon targeting both EZH1 and EZH2, we can now say definitively that both proteins possess compensatory methylase activities in vivo. Although we cannot exclude an additional methylation-independent role of EZH1 in gene control, as proposed by Margueron et al. (2008), it is notable that, like EZH2, loss of EZH1 alone also resulted in a normal postnatal skin phenotype. In contrast, here we show that loss of both EZH1 and EZH2 results in a striking arrest of HF and SG development, with progressive degeneration of these tissues. These findings underscore functional redundancy between EZH2 and EZH1 in controlling skin homeostasis.

How similar or different are the roles of the Polycomb complex in governing pluripotent ESCs in vitro and tissue-specific skin SCs in vivo? In ESCs, the Polycomb complex appears to be required for differentiation, as, upon retinoid acid stimulation, *Suz12*- and/or *Jarid2*-null ESCs fail to differentiate toward the neuronal lineage. This feature has been attributed to the failure of PcG-deficient ESCs to down-regulate stemness genes (Pasini et al. 2007, 2010). Our data show that, for several weeks, *Ezh1/2* double-knockout skin progenitors in vivo still down-regulate skin stemness genes, undergo specification of spatially and temporally defined lineages, and execute their terminal differentiation programs. These findings show that the early consequences of PcG deficiency are rooted in other aspects of tissue homeostasis, and that, postnatally, skin progenitors maintain stemness and differentiation programs, at least for a while, with either low or no PcG silencing.

Despite these differences between PcG-dependent regulation of ESCs and tissue-specific skin SCs, we also observed some similarities. In ESCs, H3K27me3 represses genes encoding key transcriptional regulators of multiple developmental lineages (Boyer et al. 2006; Margueron et al. 2008; Shen et al. 2008). Intriguingly, many of the same genes are targeted by H3K27me3 in postnatal epidermal and HF progenitor cells. Since the majority of these genes are never expressed in cells of the skin lineage, this indicates that, as in ESCs, the PcG complex globally represses multiple developmental lineages in skin progenitors. More importantly, *Ezh1/2* double-knockout skin progenitors showed, in some cases, >80-

fold increases in transcript levels of the nonskin PcG-regulated genes. That said, these levels were still dramatically low relative to their natural lineages. Thus, our findings underscore the importance, pointed out previously (Ezhkova et al. 2009), of tissue-specific transcription factors in fully activating PcG target genes.

The advantage of focusing on in vivo consequences of ablating H3K27me3 is that we could superimpose the molecular biology of epigenetics on physiological relevance to tissue homeostasis. In this regard, the most striking abnormality in *Ezh1/2*-null skin was the progressive and complete loss of regenerative capability of the HF lineage. We traced these tissue defects to markedly decreased proliferation and increased apoptosis. Moreover and intriguingly, despite the myriad of H3K27me3-repressed genes, these aberrations were largely rooted in ectopic activation of the *Ink4a/Arf/Ink4b* locus in HF cells. In culture, *Ezh1/2* double-knockout HF progenitors also failed to proliferate and survive, features that were largely overcome by repressing the locus.

Loss of the PRC1 component *Bmi1* in neural and hematopoietic lineages has been shown previously to result in activation of *Ink4a/Arf* genes. Interestingly, however, while activation occurred in both the SCs and their proliferative progenitors, self-renewal defects were confined to the SCs (Molofsky et al. 2003; Park et al. 2003). In this regard, it was surprising that, in *Ezh1/2*-null HFs, activation of the *Ink4b/Ink4a/Arf* genes led to impaired proliferation not only in the SCs, but also in their TA progeny: matrix cells. Whether this is due to tissue-specific variation or the fact that *Bmi1* ablation does not alter H3K27me3—while *Ezh1/2* ablation abolishes this epigenetic mark—awaits future investigation. Importantly, our studies show that PcG regulation of the *Ink4a/Arf/Ink4b* locus can no longer be viewed as purely an SC regulatory circuit, and they further reveal a new-found role of both EZH2 and EZH1 in governing this locus.

Perhaps the most surprising finding of our study was that the global loss of H3K27me3 did not cause widespread differentiation defects in the epidermis or HF. Thus, even though many PcG-repressed differentiation genes (Boyer et al. 2006; Lee et al. 2006; Schwartz et al. 2006) showed signs of transcriptional activation in the absence of *Ezh1/2*, the levels of nonepidermal/HF differentiation programs were still too low to reroute already established skin fates. For the epidermis, this was true even after long-term propagation by engraftment. These results are intriguing in light of *Drosophila* loss-of-Polycomb-function mutations, which also show no global effects on differentiation programs, even though they lead to homeotic transformations (Schwartz et al. 2006). The startlingly small numbers of genes that appear to be dramatically up-regulated upon loss of H3K27Me3 stand in stark contrast to the remarkably large number of genes that are decorated by this repressive histone mark. Such findings underscore the importance of additional epigenetic modifiers and backup mechanisms (other repressive histone marks, DNA methylation, and noncoding RNAs) that appear to have evolved in complex organisms to

ensure the reinforcement and maintenance of lineage programs in their adult tissues.

Materials and methods

Mice, grafts, BrdU injections, and barrier and dehydration assays

Mice were housed in the Association for Assessment and Accreditation of Laboratory Animal Care accredited animal facility at The Rockefeller University in accordance with university and NIH guidelines. Mice conditionally ablated for *Ezh2* in K14-expressing tissues of skin were reported previously (Ezhkova et al. 2009). Ezh1 knockout mice were obtained from Thomas Jenuwein's laboratory and will be reported elsewhere. Genotyping was confirmed by PCR of tail skin DNAs. Grafting procedures were essentially as described previously (Nowak et al. 2008). BrdU (Sigma-Aldrich) was administered to pregnant mice or neonatal pups by peritoneal injection (50 μ g/g BrdU). Dye exclusion assays were performed as described (Hardman et al. 1998).

Microarray analysis

RNAs from FACS-purified wild-type and *Ezh1/2* double-knockout ORS, matrix, and epidermal cells (Rendl et al. 2005) were provided to the Genomics Core Facility at Memorial Sloan-Kettering Cancer Center for quality control, quantification, reverse transcription, labeling, and hybridization to MOE430A 2.0 microarray chips (Affymetrix). Arrays were scanned per the manufacturer's specifications for the Affymetrix MOE430v2 chip. Images were background-subtracted. Probe sets were identified as differentially expressed when the absolute fold change was ≥ 2 . Probe sets selected for visualization were log₂ transformed, analyzed with hierarchical clustering (Pearson correlation, average linkage), and visualized with heat maps to assist in interpretation.

Accession numbers

Microarray data of genes expressed in wild-type and *Ezh1/2* double-knockout cells have been deposited to the Gene Expression Omnibus repository under series accession number GSE26616.

Statistics

For all graphs, mean value \pm one standard deviation was presented with the number of replicates indicated in the figure legends. To determine the significance between two groups (as indicated in the figures by a bracket), comparisons were made using Student's *t*-test. For all statistical tests, the 0.05 level of confidence was accepted for statistical significance.

ChIP assays/ChIP-seq

ChIP assay/ChIP-seq was performed as described by Cole et al. (2008) and Marson et al. (2008) and will be reported elsewhere.

Acknowledgments

The Ezh1 mutant mice were generated at the Research Institute of Molecular Pathology (IMP, Vienna) by Donal O'Carroll (laboratory of Thomas Jenuwein) with the help of Maria Sibilja (laboratory of Erwin Wagner). We also thank Alexander Tarakhovsky for previously providing us with *Ezh2* floxed mice,

and for long-standing discussions regarding aspects of PcG-mediated repression. We also thank Maria Nikolova, June Racelis, Svetlana Mazel, Lisa Polak, Dan Oristian, Christopher Bare, and Agnes Viale for technical assistance. We are grateful to Rick Young and Lee Lawton (Whitehead Institute) for their valuable assistance in ChIP-seq techniques, and Deyou Zheng (Albert Einstein College of Medicine) for ChIP-seq analyses, which will be presented in depth at a later date. We are grateful to colleagues at Rockefeller University (especially Alexander Tarakhovsky) and in the Fuchs laboratory, especially Ya-Chieh Hsu and Scott Williams, for constructive discussion, criticism, and experimental suggestions. E.E. was a New York Stem Cell Foundation post-doctoral fellow of the Life Sciences Research Foundation, and receives support from an NIH/NIAMS K99/R00 Pathway to Independence Award (1K99AR057817-01). W.H.L. is supported by a Harvey L. Karp Post-doctoral Fellowship. E.F. is an HHMI Investigator. This work was supported by grants (to E.F.) from the NIH (R01-AR050452 and R01-AR31737).

References

- Barrandon Y, Green H. 1987. Three clonal types of keratinocyte with different capacities for multiplication. *Proc Natl Acad Sci* **84**: 2302–2306.
- Barski A, Cuddapah S, Cui K, Roh TY, Schones DE, Wang Z, Wei G, Chepelev I, Zhao K. 2007. High-resolution profiling of histone methylations in the human genome. *Cell* **129**: 823–837.
- Blanpain C, Fuchs E. 2009. Epidermal homeostasis: a balancing act of stem cells in the skin. *Nat Rev Mol Cell Biol* **10**: 207–217.
- Blanpain C, Lowry WE, Geoghegan A, Polak L, Fuchs E. 2004. Self-renewal, multipotency, and the existence of two cell populations within an epithelial stem cell niche. *Cell* **118**: 635–648.
- Boyer LA, Plath K, Zeitlinger J, Brambrink T, Medeiros LA, Lee TI, Levine SS, Wernig M, Tajonar A, Ray MK, et al. 2006. Polycomb complexes repress developmental regulators in murine embryonic stem cells. *Nature* **441**: 349–353.
- Cao R, Wang L, Wang H, Xia L, Erdjument-Bromage H, Tempst P, Jones RS, Zhang Y. 2002. Role of histone H3 lysine 27 methylation in Polycomb-group silencing. *Science* **298**: 1039–1043.
- Cao R, Tsukada Y, Zhang Y. 2005. Role of Bmi-1 and Ring1A in H2A ubiquitylation and Hox gene silencing. *Mol Cell* **20**: 845–854.
- Chen H, Gu X, Su IH, Bottino R, Contreras JL, Tarakhovsky A, Kim SK. 2009. Polycomb protein Ezh2 regulates pancreatic β -cell Ink4a/Arf expression and regeneration in diabetes mellitus. *Genes Dev* **23**: 975–985.
- Cole MF, Johnstone SE, Newman JJ, Kagey MH, Young RA. 2008. Tcf3 is an integral component of the core regulatory circuitry of embryonic stem cells. *Genes Dev* **22**: 746–755.
- Cotsarelis G, Sun TT, Lavker RM. 1990. Label-retaining cells reside in the bulge area of pilosebaceous unit: implications for follicular stem cells, hair cycle, and skin carcinogenesis. *Cell* **61**: 1329–1337.
- Ezhkova E, Pasolli HA, Parker JS, Stokes N, Su IH, Hannon G, Tarakhovsky A, Fuchs E. 2009. Ezh2 orchestrates gene expression for the stepwise differentiation of tissue-specific stem cells. *Cell* **136**: 1122–1135.
- Francis NJ, Kingston RE, Woodcock CL. 2004. Chromatin compaction by a polycomb group protein complex. *Science* **306**: 1574–1577.
- Hardman MJ, Sisi P, Banbury DN, Byrne C. 1998. Patterned acquisition of skin barrier function during development. *Development* **125**: 1541–1552.

- Horsley V, O'Carroll D, Tooze R, Ohinata Y, Saitou M, Obukhanych T, Nussenzweig M, Tarakhovskiy A, Fuchs E. 2006. Blimp1 defines a progenitor population that governs cellular input to the sebaceous gland. *Cell* **126**: 597–609.
- Huang DW, Sherman BT, Lempicki RA. 2009. Systematic and integrative analysis of large gene lists using DAVID bioinformatics resources. *Nat Protoc* **4**: 44–57.
- Ito M, Yang Z, Andl T, Cui C, Kim N, Millar SE, Cotsarelis G. 2007. Wnt-dependent de novo hair follicle regeneration in adult mouse skin after wounding. *Nature* **447**: 316–320.
- Kaufman CK, Zhou P, Pasolli HA, Rendl M, Bolotin D, Lim KC, Dai X, Alegre ML, Fuchs E. 2003. GATA-3: an unexpected regulator of cell lineage determination in skin. *Genes Dev* **17**: 2108–2122.
- Lee TI, Jenner RG, Boyer LA, Guenther MG, Levine SS, Kumar RM, Chevalier B, Johnstone SE, Cole MF, Isono K, et al. 2006. Control of developmental regulators by Polycomb in human embryonic stem cells. *Cell* **125**: 301–313.
- Levy V, Lindon C, Harfe BD, Morgan BA. 2005. Distinct stem cell populations regenerate the follicle and interfollicular epidermis. *Dev Cell* **9**: 855–861.
- Levy V, Lindon C, Zheng Y, Harfe BD, Morgan BA. 2007. Epidermal stem cells arise from the hair follicle after wounding. *FASEB J* **21**: 1358–1366.
- Lewis EB. 1978. A gene complex controlling segmentation in *Drosophila*. *Nature* **276**: 565–570.
- Margueron R, Li G, Sarma K, Blais A, Zavadij J, Woodcock CL, Dynlacht BD, Reinberg D. 2008. Ezh1 and Ezh2 maintain repressive chromatin through different mechanisms. *Mol Cell* **32**: 503–518.
- Marson A, Foreman R, Chevalier B, Bilodeau S, Kahn M, Young RA, Jaenisch R. 2008. Wnt signaling promotes reprogramming of somatic cells to pluripotency. *Cell Stem Cell* **3**: 132–135.
- Min J, Zhang Y, Xu RM. 2003. Structural basis for specific binding of Polycomb chromodomain to histone H3 methylated at Lys 27. *Genes Dev* **17**: 1823–1828.
- Molofsky AV, Pardal R, Iwashita T, Park IK, Clarke MF, Morrison SJ. 2003. Bmi-1 dependence distinguishes neural stem cell self-renewal from progenitor proliferation. *Nature* **425**: 962–967.
- Nowak JA, Polak L, Pasolli HA, Fuchs E. 2008. Hair follicle stem cells are specified and function in early skin morphogenesis. *Cell Stem Cell* **3**: 33–43.
- Park IK, Qian D, Kiel M, Becker MW, Pihalja M, Weissman IL, Morrison SJ, Clarke MF. 2003. Bmi-1 is required for maintenance of adult self-renewing haematopoietic stem cells. *Nature* **423**: 302–305.
- Pasini D, Bracken AP, Hansen JB, Capillo M, Helin K. 2007. The polycomb group protein Suz12 is required for embryonic stem cell differentiation. *Mol Cell Biol* **27**: 3769–3779.
- Pasini D, Cloos PA, Walfridsson J, Olsson L, Bukowski JP, Johansen JV, Bak M, Tommerup N, Rappsilber J, Helin K. 2010. JARID2 regulates binding of the Polycomb repressive complex 2 to target genes in ES cells. *Nature* **464**: 306–310.
- Pereira JD, Sansom SN, Smith J, Dobenecker MW, Tarakhovskiy A, Livesey FJ. 2010. Ezh2, the histone methyltransferase of PRC2, regulates the balance between self-renewal and differentiation in the cerebral cortex. *Proc Natl Acad Sci* **107**: 15957–15962.
- Rendl M, Lewis L, Fuchs E. 2005. Molecular dissection of mesenchymal–epithelial interactions in the hair follicle. *PLoS Biol* **3**: e331. doi: 10.1371/journal.pbio.0030331.
- Ringrose L, Paro R. 2004. Epigenetic regulation of cellular memory by the Polycomb and Trithorax group proteins. *Annu Rev Genet* **38**: 413–443.
- Sarma K, Margueron R, Ivanov A, Pirrotta V, Reinberg D. 2008. Ezh2 requires PHF1 to efficiently catalyze H3 lysine 27 trimethylation in vivo. *Mol Cell Biol* **28**: 2718–2731.
- Sauvageau M, Sauvageau G. 2010. Polycomb group proteins: multi-faceted regulators of somatic stem cells and cancer. *Cell Stem Cell* **7**: 299–313.
- Schneider MR, Schmidt-Ullrich R, Paus R. 2009. The hair follicle as a dynamic miniorgan. *Curr Biol* **19**: R132–R142. doi: 10.1016/j.cub.2008.12.005.
- Schwartz YB, Kahn TG, Nix DA, Li XY, Bourgon R, Biggin M, Pirrotta V. 2006. Genome-wide analysis of Polycomb targets in *Drosophila melanogaster*. *Nat Genet* **38**: 700–705.
- Shen X, Liu Y, Hsu YJ, Fujiwara Y, Kim J, Mao X, Yuan GC, Orkin SH. 2008. EZH1 mediates methylation on histone H3 lysine 27 and complements EZH2 in maintaining stem cell identity and executing pluripotency. *Mol Cell* **32**: 491–502.
- Sherr CJ, Roberts JM. 2004. Living with or without cyclins and cyclin-dependent kinases. *Genes & Dev* **18**: 2699–2711.
- Simon JA, Kingston RE. 2009. Mechanisms of polycomb gene silencing: knowns and unknowns. *Nat Rev Mol Cell Biol* **10**: 697–708.
- Su IH, Basavaraj A, Krutchinsky AN, Hobert O, Ullrich A, Chait BT, Tarakhovskiy A. 2003. Ezh2 controls B cell development through histone H3 methylation and Igh rearrangement. *Nat Immunol* **4**: 124–131.
- Su IH, Dobenecker MW, Dickinson E, Oser M, Basavaraj A, Marqueron R, Viale A, Reinberg D, Wulfe C, Tarakhovskiy A. 2005. Polycomb group protein ezh2 controls actin polymerization and cell signaling. *Cell* **121**: 425–436.
- Trempus CS, Morris RJ, Bortner CD, Cotsarelis G, Faircloth RS, Reece JM, Tennant RW. 2003. Enrichment for living murine keratinocytes from the hair follicle bulge with the cell surface marker CD34. *J Invest Dermatol* **120**: 501–511.
- Tumbar T, Guasch G, Greco V, Blanpain C, Lowry WE, Rendl M, Fuchs E. 2004. Defining the epithelial stem cell niche in skin. *Science* **303**: 359–363.
- Vidal VP, Ortonne N, Schedl A. 2008. SOX9 expression is a general marker of basal cell carcinoma and adnexal-related neoplasms. *J Cutan Pathol* **35**: 373–379.